Catalysis Letters Vol. 110, Nos. 3–4, September 2006 (© 2006)
DOI: 10.1007/s10562-006-0121-z

$Pt–Ni/\gamma\text{-}Al_2O_3$ catalyst for the preferential CO oxidation in the hydrogen stream

Eun-Yong Ko,[a] Eun Duck Park,[a,*] Kyung Won Seo,[a] Hyun Chul Lee,[b] Doohwan Lee,[b] and Soonho Kim[b]

[a]*Department of Chemical Engineering, Division of Chemical Engineering and Materials Engineering, Ajou University, Wonchun-Dong, Yeongtong-Gu, Suwon, 443-749, Republic of Korea*

[b]*Energy & Materials Research Laboratory, Samsung Advanced Institute of Technology (SAIT), P.O. Box 111 Suwon, 440-600, Republic of Korea*

Received 22 February 2006; accepted 26 June 2006

The preferential CO oxidation (PROX) in the presence of excess hydrogen was studied over $Pt–Ni/\gamma\text{-}Al_2O_3$. CO chemisorption, X-ray diffraction, transmission electron microscopy, energy dispersive X-ray spectroscopy and temperature-programmed reduction were conducted to characterize active catalysts. The co-impregnated $Pt–Ni/\gamma\text{-}Al_2O_3$ was superior to $Pt/Ni/\gamma\text{-}Al_2O_3$ and $Ni/Pt/\gamma\text{-}Al_2O_3$ prepared by a sequential impregnation of each component on alumina support. The PROX activity was affected by the reductive pretreatment condition. The pre-reduction was essential for the low-temperature PROX activity. As the reduction temperature increased above 423 K, the CO_2 selectivity decreased and the atomic percent of Ni in the bimetallic phase of Pt–Ni increased. This catalyst exhibited the high CO conversion even in the presence of 2% H_2O and 20% CO_2 over a wide reaction temperature. The bimetallic phase of Pt–Ni seems to give rise to high catalytic activity for the PROX in H_2-rich stream.

KEY WORDS: CO oxidation; PROX; $Pt/\gamma\text{-}Al_2O_3$; Pt–Ni; fuel cell.

1. Introduction

The polymer electrolyte membrane fuel cell (PEMFC) which has been attracting much attention in the application of electric vehicles or residential power generations produces heat and electricity with the hydrogen fuel that can be generated via reforming of hydrocarbons followed by water-gas shift (WGS) reaction [1]. However, the low catalytic reactivity of the current WGS catalyst limits a complete carbon monoxide (CO) conversion which can be accomplished thermodynamically at low temperatures. Consequently, 0.5–1.0 vol.% of unconverted CO is usually remained in the hydrogen fuel at the downstream of WGS reactor. This CO should be removed to a trace-level because platinum, an anode of PEMFC, can be easily poisoned by small amounts of CO in hydrogen stream. The acceptable CO concentration reported in the literature is below 100 ppm even at CO-tolerant anodes [2]. The preferential CO oxidation (PROX) has been accepted as the most attractive way to reduce CO concentration. In this system, the following three reactions can occur.

$$\text{CO oxidation: } CO + 1/2O_2 \rightarrow CO_2 \quad (1)$$

$$H_2 \text{ oxidation: } H_2 + 1/2O_2 \rightarrow H_2O \quad (2)$$

$$\text{CO hydrogenation: } CO + 3H_2 \rightarrow CH_4 + H_2O \quad (3)$$

The third reaction, which is called methanation, should be avoided except when CO concentration was quite low because it consumed relatively large amounts of hydrogen compared with the PROX. Although a number of catalysts more active for the PROX than the H_2 oxidation reaction have been reported [2–19], CuO–CeO_2 and supported Pt-based catalysts appear to be most promising [2,3]. The monometallic Pt catalyst usually showed noticeable activities only above 423 K [6]. Because PEMFC is operated below 423 K, catalysts operating at low temperatures can be more plausible for practical applications. To increase catalytic activities at low temperatures, various methods have been tried in the preparation of supported Pt catalysts. The pretreatment of Pt catalyst with water vapor was reported to enhance low-temperature catalytic activities for the PROX by increasing Pt dispersion [7]. Several groups have reported that the PROX at low temperatures could be enhanced by the addition of 2nd metals such as Ce [8], Fe [9–12], Co [13–16], Ni [13], Mn [13], and alkali metals [17–19]. Even though each catalyst has proved its superiority by comparison with Pt catalyst, it is difficult to assess each catalyst because different reaction conditions have been adopted. In our previous work, we reported a comparative CO oxidation study using various promoted Pt catalysts at the same reaction condition and found that the addition of Ni was the most effective for the PROX [20]. In this study, the effect of impregnation sequences and pretreatment conditions on the catalytic activity over Ni-promoted $Pt/\gamma\text{-}Al_2O_3$

---

*To whom correspondence should be addressed.
E-mail: edpark@ajou.ac.kr

catalyst was examined. The comparison with other PROX catalysts was also conducted.

2. Experimental

Pt/γ-Al_2O_3 and Pt–Ni/γ-Al_2O_3 catalysts was prepared by a wet impregnation method from an aqueous solution of $Pt(NH_3)_4(NO_3)_2$ and/or $Ni(NO_3)_2$. Pt/Ni/γ-Al_2O_3 and Ni/Pt/γ-Al_2O_3 was prepared by a sequential impregnation method with Ni/γ-Al_2O_3 and Pt/γ-Al_2O_3 both pretreated with air at 573 K. γ-Al_2O_3 (Alfa) was utilized as a support. The content of Pt and Ni was 1.0 wt.% and 1.5 wt.%, respectively. For comparison, CuO–CeO_2 catalyst containing 20 mol% Cu was prepared by a co-precipitation method and used after calcinations at 773 K.

Bulk crystalline structures of catalysts were determined with an X-ray diffraction (XRD) technique. XRD patterns were obtained by using Cu-Kα radiation using a Rigaku D/MAC-III instrument at room temperature.

Temperature programmed reduction (TPR) was conducted over 0.2 g sample in a 10 vol.% H_2/Ar stream from 313 K to 773 K at a heating rate 10 K/min monitoring TCD signals after samples were pretreated with air at 573 K for 1 h.

The CO chemisorption was conducted over 0.2 g sample in a He stream at 300 K by a pulsed injection of 50 μL of CO after samples were pretreated at different conditions.

The bright-field image of transmission electron microscopy (TEM) was obtained using a Technai G^2 TEM (FEI) operated at 200 kV. Samples were finely ground in a mortar to fine particles and then dispersed ultrasonically in methanol. The sample was deposited on a Cu grid covered by a holey carbon film for measurements. Energy dispersive X-ray spectroscopy (EDX) was also conducted.

Experiments were carried out in a small fixed bed reactor with catalysts that had been retained between 45 and 80 mesh sieves. A standard gas of 1.0 vol.% CO, 1.0 vol.% O_2, 2 vol.% H_2O and 80 vol.% H_2 balanced with helium was fed to the reactor at an atmospheric pressure. The catalytic activity with increasing reaction temperature was measured from 313 K to 473 K at a ramping rate of 1 K/min. The effect of H_2O and CO_2 was examined with a gas mixture of 1.0 vol.% CO, 1.0 vol.% O_2, 2 vol.% H_2O, 20 vol.% CO_2, and 50 vol.% H_2 balanced with helium. In this case, the steady-state data were obtained at each reaction temperature. For all experiments, 0.10 g of catalyst without diluents was contacted with a reactant gas at a flow rate of 100 mL/min. The conversion of CO and O_2 and the yield of CH_4 were determined through gas chromatographic analysis (HP5890A, molecular sieve 5A column) of the effluent from the reactor. The detection limit of CO was 10 ppm. The CO conversion, O_2 conversion, CO_2 selectivity, and the CH_4 yield were calculated using the following formulas:

$$\text{CO conversion}(\%) = \{([\text{CO}]_{\text{in}} - [\text{CO}]_{\text{out}})/[\text{CO}]_{\text{in}}\} \times 100;$$

$$\text{O}_2 \text{ conversion}(\%) = \{([\text{O}_2]_{\text{in}} - [\text{O}_2]_{\text{out}})/[\text{O}_2]_{\text{in}}\} \times 100;$$

$$\text{CO}_2 \text{ selectivity}(\%) = \{0.5 \times ([\text{CO}]_{\text{in}} - [\text{CO}]_{\text{out}} - [\text{CH}_4]_{\text{out}})/([\text{O}_2]_{\text{in}} - [\text{O}_2]_{\text{out}})\} \times 100;$$

$$\text{CH}_4 \text{ yield } (\%) = ([\text{CH}_4]_{\text{out}})/[\text{CO}]_{\text{in}}) \times 100.$$

3. Results and discussion

The BET surface area of γ-Al_2O_3 calculated using N_2 adsorption isotherm was 170 m^2/g. Ni-promoted Pt/γ-Al_2O_3 catalysts prepared by various impregnation sequences of Pt and Ni were examined for the PROX in the presence of excess hydrogen as shown in figure 1. The extremely high H_2 concentration (80 vol.%) in the reactant stream was adopted to compare catalytic activities among catalysts composed of the same catalyst composition. Compared with those in Pt/γ-Al_2O_3, the

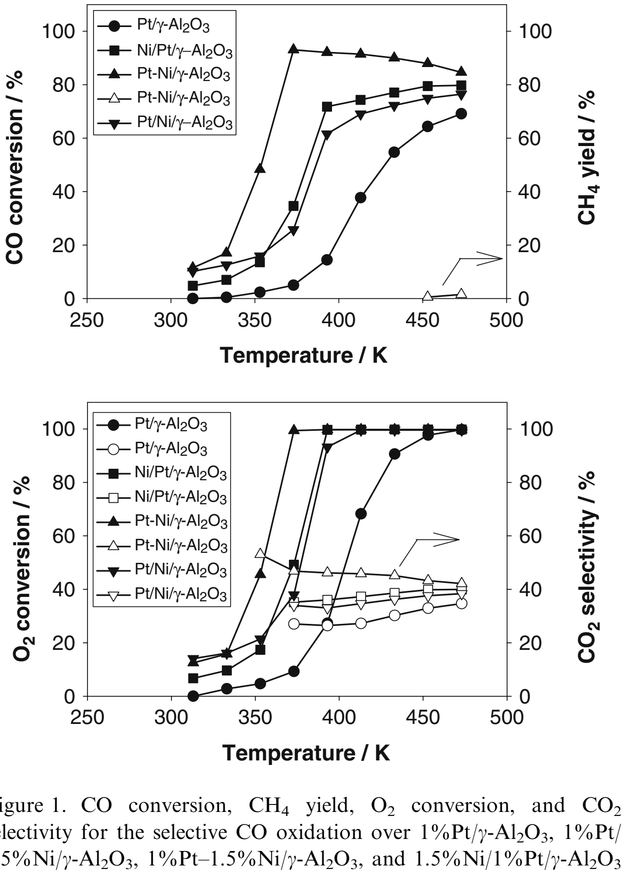

Figure 1. CO conversion, CH_4 yield, O_2 conversion, and CO_2 selectivity for the selective CO oxidation over 1%Pt/γ-Al_2O_3, 1%Pt/1.5%Ni/γ-Al_2O_3, 1%Pt–1.5%Ni/γ-Al_2O_3, and 1.5%Ni/1%Pt/γ-Al_2O_3 with increasing reaction temperature. All catalysts were calcined with air at 573 K and reduced with H_2 at 573 K before a reaction. Reactants: 1% CO, 1% O_2, 80% H_2, and 2% H_2O in He. *F*/*W* = 1000 mL/min/g_{cat}.

addition of Ni to Pt/γ-Al_2O_3 catalyst resulted in a greatly enhanced CO conversion as well as O_2 conversion at all reaction temperatures irrespective of the preparation sequence. Among Ni-promoted Pt/γ-Al_2O_3 catalysts, the co-impregnated Pt–Ni/γ-Al_2O_3 showed the highest CO and O_2 conversion at all reaction temperatures. Ni/Pt/γ-Al_2O_3 was slightly more active than Pt/Ni/γ-Al_2O_3 for the PROX at temperatures above 373 K. The CO_2 selectivity follows the order: Pt–Ni/γ-Al_2O_3 > Ni/Pt/γ-Al_2O_3 > Pt/Ni/γ-Al_2O_3 > Pt/γ-Al_2O_3. The CO methanation was observed over Pt–Ni/γ-Al_2O_3 at temperatures above 453 K whereas it was not detected over other catalysts.

In order to find out the reason of the improved catalytic performance for the PROX over Ni-promoted Pt/γ-Al_2O_3 catalysts, the interactions between Pt and Ni as well as those between metal species and the support were investigated by the temperature programmed reduction (TPR). Figure 2 shows these TPR patterns of γ-Al_2O_3-supported monometallic Pt and Ni catalysts as well as Ni-promoted Pt/γ-Al_2O_3 catalysts. As can be seen in figure 2, Pt/γ-Al_2O_3 catalyst showed a broad reduction peak around 465 K, which can be assigned to the reduction of platinum oxide into the metallic Pt. Ni/γ-Al_2O_3 catalyst exhibited two reduction peaks around 520 K and 570 K. These reduction peaks which appeared to be overlapped originated from the reduction of NiO into the metallic Ni and disappeared in all Ni-promoted Pt/γ-Al_2O_3 catalysts as revealed in figure 2. A sharp new reduction peak around 430 K was observed in all Ni-promoted Pt/γ-Al_2O_3 catalysts with a broad tailing peak around 465 K. This reduction started at the lowest temperature over Pt–Ni/γ-Al_2O_3 catalyst. Compared with those of Pt/γ-Al_2O_3 and Ni/γ-Al_2O_3, the reduction of metal oxides occurred at much lower temperatures for all Ni-promoted Pt/γ-Al_2O_3 catalyst. This can be interpreted that new metal oxide composed of Pt and Ni was formed in the calcinations step. This Pt–Ni oxide must be reduced at lower temperature than PtO_x or NiO. Furthermore, this mixed metal oxide can be easily made with a co-impregnation method. Based on the correlation between the onset of reduction in TPR patterns and the catalytic activity, the bimetallic phase of Pt–Ni should play an important role in the PROX, especially at low temperatures. For all Ni-promoted Pt/γ-Al_2O_3 catalyst, the peak due to reduction of NiO could not be observed around 570 K. This can be interpreted that NiO was reduced at much lower temperature such as 430 K in the presence of Pt and Pt–Ni which accelerates the dissociation of molecular hydrogen. This shift in reduction temperature of metal oxides in the presence of noble metals such as Pt and Ru was also reported in supported cobalt oxide system [21–23]. A very small amount of continuous H_2 consumption was observed till 1000 K in TPR pattern for Ni-containing samples. This can be originated from reduction of surface nickel aluminate ($NiAl_2O_4$). The slight difference in total H_2 consumption can be due to differences in the amount of $NiAl_2O_4$.

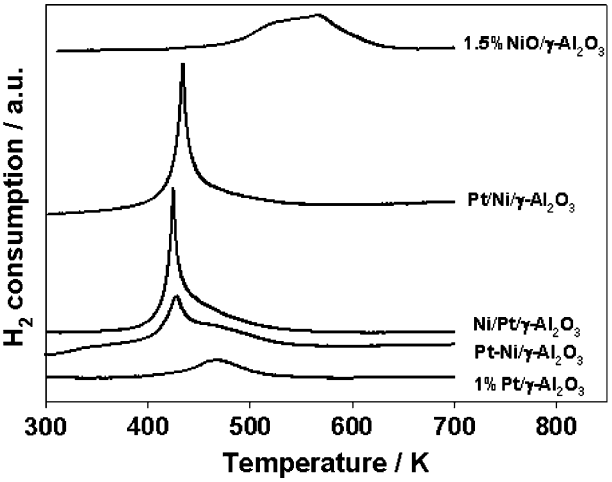

Figure 2. TPR patterns of 1%Pt/γ-Al_2O_3, 1%Pt/1.5%Ni/γ-Al_2O_3, 1%Pt–1.5%Ni/γ-Al_2O_3, 1.5%Ni/1%Pt/γ-Al_2O_3, and 1.5%Ni/γ-Al_2O_3. All catalysts were calcined with air at 573 K before an experiment.

The pretreatment effect of this Pt–Ni/γ-Al_2O_3 catalyst on the catalytic activity was examined as shown in figure 3. The unreduced Pt–Ni/γ-Al_2O_3 catalyst showed the noticeable activity only when the reaction temperature

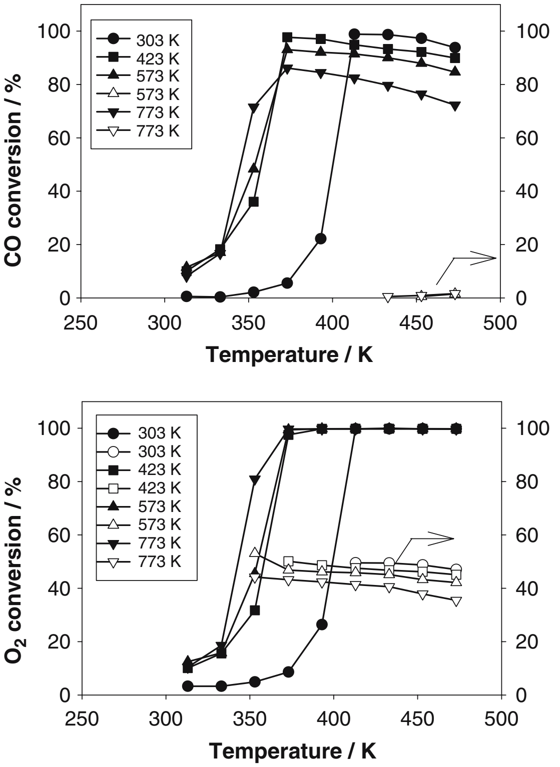

Figure 3. CO conversion, CH_4 yield, O_2 conversion, and CO_2 selectivity for the selective CO oxidation over 1%Pt–1.5%Ni/γ-Al_2O_3 catalysts calcined in air at 573 K and reduced with H_2 at different temperatures with increasing reaction temperatures. Reactants: 1% CO, 1% O_2, 80% H_2, and 2% H_2O in He. F/W = 1000 mL/min/g_{cat}.

was higher than 400 K. This is consistent with the onset reduction temperature observed in TPR pattern. That is, the bimetallic oxide phase in Pt–Ni/γ-Al_2O_3 calcined at 573 K would be reduced spontaneously as the reaction temperature increased under H_2-rich stream of reactant. When the catalytic activity of Pt–Ni/γ-Al_2O_3 calcined at 573 K was compared with that of Pt–Ni/γ-Al_2O_3 calcined at 573 K and reduced at 423 K, it could be observed that the lowest reaction temperature showing more than 90% CO conversion was shifted to the lower temperature by about 40 K. Therefore, it is obvious that the reduced bimetallic phase of Pt–Ni is responsible for high catalytic activities at low temperatures. The PROX activity and the CO_2 selectivity of this catalyst were markedly dependent on the reduction temperature. Although the CO conversion increased as the reduction temperature increased from 423 K to 773 K in the reaction temperature range below 373 K, opposite trends were observed at above 373 K as shown in figure 3.

CO chemisorption was carried out to compare the amount of surface active site of catalysts. The amount of chemisorbed CO on Pt/γ-Al_2O_3 calcined and reduced both at 573 K and Pt–Ni/γ-Al_2O_3 calcined at 573 K and reduced at 423 K was determined to be 34.8 μmol/$g_{cat.}$ and 23.9 μmol/$g_{cat.}$, respectively. This shows that the addition of Ni decreased the amount of surface active site for CO chemisorption. However, Pt–Ni/γ-Al_2O_3 was noticeably superior to Pt/γ-Al_2O_3 for the PROX. These facts support that Pt–Ni/γ-Al_2O_3 showed much higher catalytic activities than Pt/γ-Al_2O_3 based on the active site. The increasing catalytic activity for O_2 oxidation with increasing reduction temperature for Pt–Ni/γ-Al_2O_3 catalyst can be explained by the increasing active sites because Pt–Ni/γ-Al_2O_3 calcined and reduced both at 573 K was determined to be 40.4 μmol/$g_{cat.}$. The CO oxidation in the presence of excess H_2 would compete with H_2 oxidation. The bimetallic phase of Pt–Ni in Pt–Ni/γ-Al_2O_3 catalyst would facilitate the oxidation reaction with increasing reduction temperature because the amount of active site also increases. However, as the reaction temperatures increases further, the CO oxidation would be more competing with H_2 oxidation. Consequently, the CO conversion and the CO_2 selectivity decreased as a result of an enhanced activity for H_2 oxidation. Thus, it could be suggested that the bimetallic phase of Pt–Ni in Pt–Ni/γ-Al_2O_3 would reduce the activation energy for H_2 oxidation as well as that for CO oxidation.

To observe the bimetallic phase of Pt–Ni, the TEM image was obtained for Pt–Ni/γ-Al_2O_3 catalyst calcined in air at 573 K and reduced with H_2 at 423 K as shown in figure 4. The highly well-dispersed metal particles were observed as revealed in figure 4(a). The average particle size of metal particles was estimated to be 2.8 ± 0.3 nm. A representative single metal particle is shown in figure 4(b). The EDX analysis was conducted to find out the composition of the metallic particles. Two different points were selected as shown in figure 4(c). Pt and Ni were found to be present and the atomic ratio of Ni/Pt was determined to be 1.1 at point 1. However, only Ni was present and the atomic ratio of Ni/Al was analyzed to be 0.6 at point 2. Therefore, this result supports that some Ni species are present as the bimetallic phase with Pt and the remaining Ni species exist as surface $NiAl_2O_4$. For the repeated EDX analysis, the atomic ratio of Ni/Pt differed with a range of 0.5–2. Thus, the bimetallic phase with different atomic ratio of Ni/Pt would exist in Pt–Ni/γ-Al_2O_3 catalyst and this would be related with earlier onset of reduction temperature in Pt–Ni/γ-Al_2O_3 catalyst. It was found that the atomic percent of Ni in the bimetallic phase of Pt–Ni increases with increasing reduction temperatures. For Pt–Ni/γ-Al_2O_3 catalyst calcined at 573 K and reduced at 773 K, the atomic percent of Ni differed with a range of 77–94%. Thus, the Ni-enriched bimetallic phase of Pt–Ni would exist in Pt–Ni/γ-Al_2O_3 catalyst reduced at 773 K compared with that of Pt–Ni/γ-Al_2O_3 catalyst reduced at 423 K. Based on the fact that the CO_2 selectivity decreased but the atomic percent of Ni increased with increasing reduction temperature, the bulk composition in Pt–Ni bimetals must be closely related to the CO_2 selectivity.

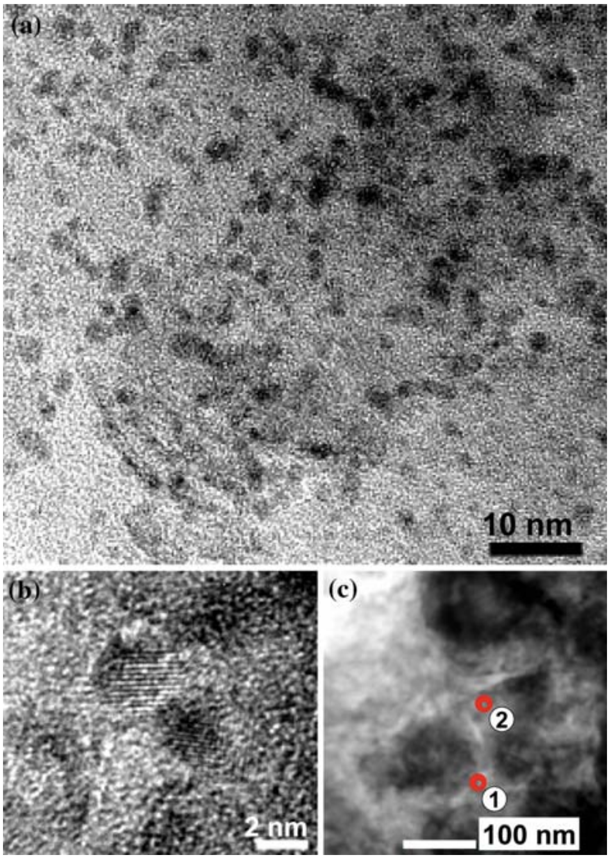

Figure 4. The bright-field TEM images (a, b) and the TEM image (c) for EDX analysis of 1%Pt–1.5%Ni/γ-Al_2O_3 catalyst calcined in air at 573 K and reduced with H_2 at 423 K.

XRD patterns were obtained to determine bulk crystalline structure of above all catalysts. However, no peak representing crystalline phase due to Pt and Ni compounds was found except peaks representing γ-Al_2O_3. Therefore, it can be assumed that these metals were present in a highly dispersed form. This was also supported by the CO chemisorption and TEM for some catalysts.

The catalytic performance of selected Pt–Ni/γ-Al_2O_3 catalyst was compared with that of other PROX catalysts such as CuO–CeO_2 and Pt/γ-Al_2O_3 catalyst as shown in figure 5. The feed composition was changed to be more practical condition including CO_2 in H_2-rich reactant stream. The concentration of hydrogen and carbon dioxide was 50 and 20 vol.%, respectively. Compared with CuO–CeO_2 and Pt/γ-Al_2O_3 catalyst, Pt–Ni/γ-Al_2O_3 catalyst showed the highest CO conversion and CO_2 selectivity over a wide reaction temperature.

4. Conclusions

Compared with that of Pt/γ-Al_2O_3 catalyst, Ni-promoted Pt/γ-Al_2O_3 catalyst showed the higher CO conversion with a higher CO_2 selectivity over a wide reaction temperature for the PROX in the presence of excess hydrogen. Among Ni-promoted Pt/γ-Al_2O_3 catalysts, the co-impregnated Pt–Ni/γ-Al_2O_3 was superior to Pt/Ni/γ-Al_2O_3 and Ni/Pt/γ-Al_2O_3 prepared by a sequential impregnation of each component on alumina support. Pt–Ni/γ-Al_2O_3 catalyst showed much lower reduction temperature than that in Pt/Ni/γ-Al_2O_3 and Ni/Pt/γ-Al_2O_3, which implies much stronger interaction between Pt and Ni and weaker metal–support interaction. The PROX activity was also affected by the reductive pretreatment condition. The pre-reduction was essential for the low-temperature PROX activity. As the reduction temperature increased above 423 K, the CO_2 selectivity decreased and the atomic percent of Ni in the bimetallic phase of Pt–Ni increased. The bimetallic phase of Pt–Ni seems to give rise to high catalytic activity for the PROX in H_2-rich stream.

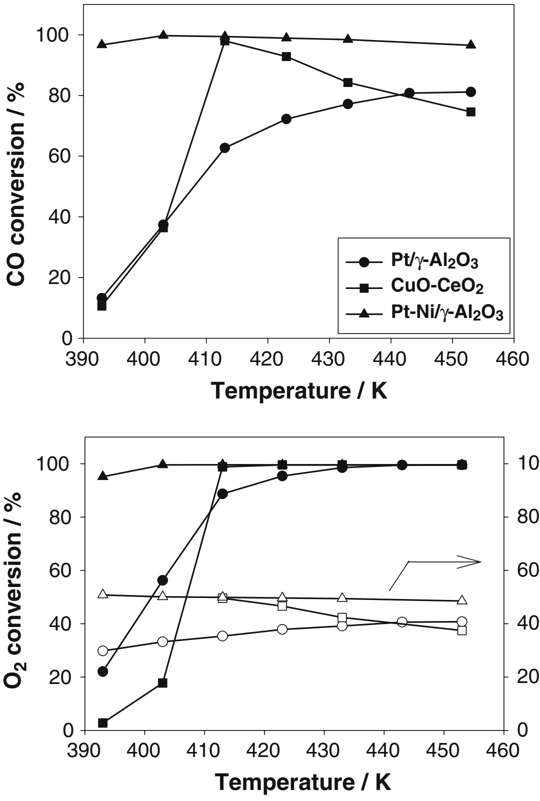

Figure 5. The steady-state CO conversion, O_2 conversion, and CO_2 selectivity for the selective CO oxidation over 1%Pt/γ-Al_2O_3 (circle), CuO–CeO_2 (square), and 1%Pt–1.5%Ni/γ-Al_2O_3 (triangle) at different temperatures. Reactants: 1% CO, 1% O_2, 50% H_2, 20%CO_2, and 2% H_2O in He. F/W = 1000 mL/min/g_{cat}.

Acknowledgment

We acknowledge financial support from the Samsung Advanced Institute of Technology (SAIT).

References

[1] C. Song, Catal. Today 77 (2002) 17.
[2] L. Shore and R.J. Farrauto, in: *Handbook of Fuel Cells: Fundamentals Technology and Applications*, W. Vielstich, A. Lamm and H.A. Gasteiger (eds.), 3(John Wiley & Sons Ltd, West Sussex, 2003) pp. 211–Part 2.
[3] S.H. Oh and R.M. Sinkevitch, J. Catal. 142 (1993) 254.
[4] R.J.H. Grisel and B.E. Nieuwenhuys, J. Catal. 199 (2001) 48.
[5] D.H. Kim and J.E. Cha, Catal. Lett. 86 (2003) 107.
[6] A. Manasilp and E. Gulari, Appl. Catal. B 37 (2002) 17.
[7] I.H. Son, M. Shamsuzzoha and A.M. Lane, J. Catal. 210 (2002) 460.
[8] I.H. Son and A.M. Lane, Catal. Lett. 76 (2001) 151.
[9] O. Korotkikh and R. Farrauto, Catal. Today 62 (2000) 249.
[10] X. Liu, O. Korotkikh and R. Farrauto, Appl. Catal. A 226 (2002) 293.
[11] M. Watanabe, H. Uchida, K. Ohkubo and H. Igarashi, Appl. Catal. B 46 (2003) 595.
[12] A. Sirijaruphan, J.G. Goodwin Jr. and R.W. Rice, J. Catal. 224 (2004) 304.
[13] D.J. Suh, C. Kwak, J.-H. Kim, S.M. Kwon and T.-J. Park, J. Power Sources 142 (2005) 70.
[14] C. Kwak, T.-J. Park and D.J. Suh, Chem. Eng. Sci. 60 (2005) 1211.
[15] C. Kwak, T.-J. Park and D.J. Suh, Appl. Catal. A 278 (2005) 181.
[16] E.-Y. Ko, E.D. Park, K.W. Seo, H.C. Lee, D. Lee, and S. Kim, J. Nanosci. Nanotechnol. in press.
[17] S.-H. Cho, J.-S. Park, S.-H. Choi and S.-H. Kim, J. Power Sources 156 (2006) 166.
[18] Y. Minemura, S. Ito, T. Miyao, S. Naito, K. Tomishige, and K. Kunimori , Chem. Commun. (2005) 1429.
[19] C. Pedrero, T. Waku and E. Iglesia, J. Catal. 233 (2005) 242.
[20] E.-Y. Ko, E.D. Park, K.W. Seo, H.C. Lee, D. Lee and S. Kim, Kor. J. Chem. Eng. 23 (2006) 182.
[21] G. Jacobs, T.K. Das, Y. Zhang, J. Li, G. Racoillet and B.H. Davis, Appl. Catal. A 233 (2002) 263.
[22] Z. Zsoldos, F. Garrin, L. Hilaire and L. Guczi, J. Mol. Catal. A. 111 (1996) 113.
[23] L. Guczi, Catal. Today 101 (2005) 53.